minerals

MDPI

Review

Metallogenic Evolution of Northeast Asia Related to the Cretaceous Turn of Geological Evolution

Victor P. Nechaev [1,*], Frederick L. Sutherland [2] and Eugenia V. Nechaeva [3]

[1] Far East Geological Institute, Far Eastern Branch, Russian Academy of Sciences, 159 Prospect 100-Letiya, 690022 Vladivostok, Russia
[2] Geoscience, Australian Museum, 1 William Street, Sydney, NSW 2010, Australia; linsutherland1@gmail.com
[3] Polytechnic Institute, Far Eastern Federal University, 690922 Vladivostok, Russia; geolog2001@yandex.ru
* Correspondence: nechaev@fegi.ru; Tel.: +79-024-866-273

Abstract: This study tests the hypothesis of Cretaceous Turn of Geological Evolution (CTGE). It uses the large dataset on mineral deposits of NE Asia compiled by the US Geological Survey in collaboration with Russian, Mongolian, Korean, and Japanese geological institutions. As predicted, the Triassic–Early Jurassic and Late Cretaceous–Paleogene geodynamic activities in NE Asia were simple, producing a relatively small amount of mineral deposits (94 and 132, respectively). In contrast, the greatly increased geodynamic activity around CTGE produced a huge amount of mineral deposits (288). The Jurassic–Early Cretaceous superplume-related melts were injected into accretionary wedges that formed along the Pacific–Eurasian margins, whereas adakitic and granitic magmas derived from the shallow slab and lower crust were intruded into the huge intracontinental region. The characteristic mineral deposits are represented by the unique Jurassic–Early Cretaceous plume-related Ti-Fe-V (+P + Cr-PGE + Au + diamond) ores. Other CTGE representatives are the porphyry Cu-Mo and Au (+Ag)-vein deposits, which formation, however, continued into the Late Cretaceous–Paleogene epoch. These deposits were generated by the slab- and crust-derived adakitic and granitic melts formed under influence of the expiring superplume and intensifying subduction. The Late Cretaceous–Paleogene epoch is indicated by a decreasing metallogenic activity in general, and an increasing role of subduction-related deposits in particular.

Keywords: Cretaceous turn of geological evolution; northeast Asia; metallogenic belts; mineral deposits; superplume; flat subduction

Citation: Nechaev, V.P.; Sutherland, F.L.; Nechaeva, E.V. Metallogenic Evolution of Northeast Asia Related to the Cretaceous Turn of Geological Evolution. *Minerals* **2022**, *12*, 400. https://doi.org/10.3390/min12040400

Academic Editor: Sung Hi Choi

Received: 21 February 2022
Accepted: 23 March 2022
Published: 24 March 2022

1. Introduction

This study examines the hypothesis of the Cretaceous turn of geological evolution (CTGE) [1,2] using the large dataset on mineral deposits and metallogenic belts of NE Asia that was compiled by the US Geological Survey in collaboration with the Russian Academy of Sciences, Mongolian Academy of Sciences, Jilin University (Changchun Branch), Korean Institute of Geology, Mining, and Materials, and Geological Survey of Japan/AIST [3,4].

The hypothesis suggests that "the galactic seasons of the Earth indicate significant changes caused by its distance from the Sun while that star was in transit along its elliptical orbit" [5]. According to references [1,2], the Solar System periodically passes through critical points of its galactic orbit (apo- and pericenters) that should lead to some global phases of geological evolution. The last event of this kind happened in the Early Cretaceous (around 135 Ma) when our star (the Sun) likely passed the apocenter, the most distant point of its galactic orbit. During this event, the Earth underwent maximum extension, associated with its relative closeness to the Sun and then long-term contraction related to its distancing. In addition, a liquid nature of the Earth's core reacted to the gravitational and electromagnetic changes in the nearest part of the Universe. Turbulent flows in the outer core favored the rise of voluminous magmatic plumes and associated fluid flows. The plumes and flows

substantially transformed the mantle, crust, hydrosphere, biosphere, and atmosphere [1,2]. These, with associated juvenile events, produced numerous metallic ore, coal, gas, and oil deposits. This study presents evidence of this anomalously high metallogenic activity that has made the Cretaceous one of the most significant resource-producing periods in the Earth's history.

The present study includes data from a key region of Cretaceous magmatic and mineralization activity involving adakite rock suites within an indicated East Asian adakite province. Adakite rocks now encompass a range of defined characteristics and genetic interpretations within their petrologic make up and a brief synopsis of their nature and tectonic applications is presented here. The term adakite originally described siliceous arc igneous rocks with distinctive chemical compositions having low Y and Yb values and high Sr/Y, La/Yb ratios and were thought to represent melting of young, subducted ocean floor. In later studies their geochemistry widened and these adakite-like lithologies invoked other proposed genetic models [6,7].

2. Sources of Data and Methods of Interpretation

The consulted metallogenic reviews of NE Asia [3,4] have gathered information on many hundred mineral deposits for a very large region (Figures 1–3) and provide a unique platform to undertake the task of this study. These reports not only classified data on the deposits based on their age, commodity, size, genesis, and geographic location, but also grouped the deposits into metallogenic belts associated with various magmatic units related to different geodynamic settings. The latter include collision/accretion-, subduction-, transform plate boundary-, and plume-related settings.

To interpret the data for better correlation, the DATABASE by [3] (https://pubs.usgs.gov/of/2003/of03-220/DATABASE/, accessed on 23 March 2022) was reorganized into an Excel file (Supplementary Table S1) that may be downloaded from the MINERALS website. In the table, the lode deposits are grouped into three age ranges, particularly Late Triassic–Early Cretaceous (230–175 Ma), Middle Jurassic–Early Cretaceous (175–96 Ma), and Late Cretaceous–Paleogene (96–24 Ma). Note that numerical ages of the metallogenic epochs, which are used after [3], do not accurately represent subdivisions of the modern International Stratigraphic Chart (www.stratigraphy.org, accessed on 20 February 2022). However, they roughly correspond to the galactic seasonality [1,2]. In particular, the time interval of 230–175 Ma corresponds to the galactic spring, 175–96 Ma to the galactic summer focusing on the CTGE time (135–120 Ma), and 96–24 Ma to the galactic autumn.

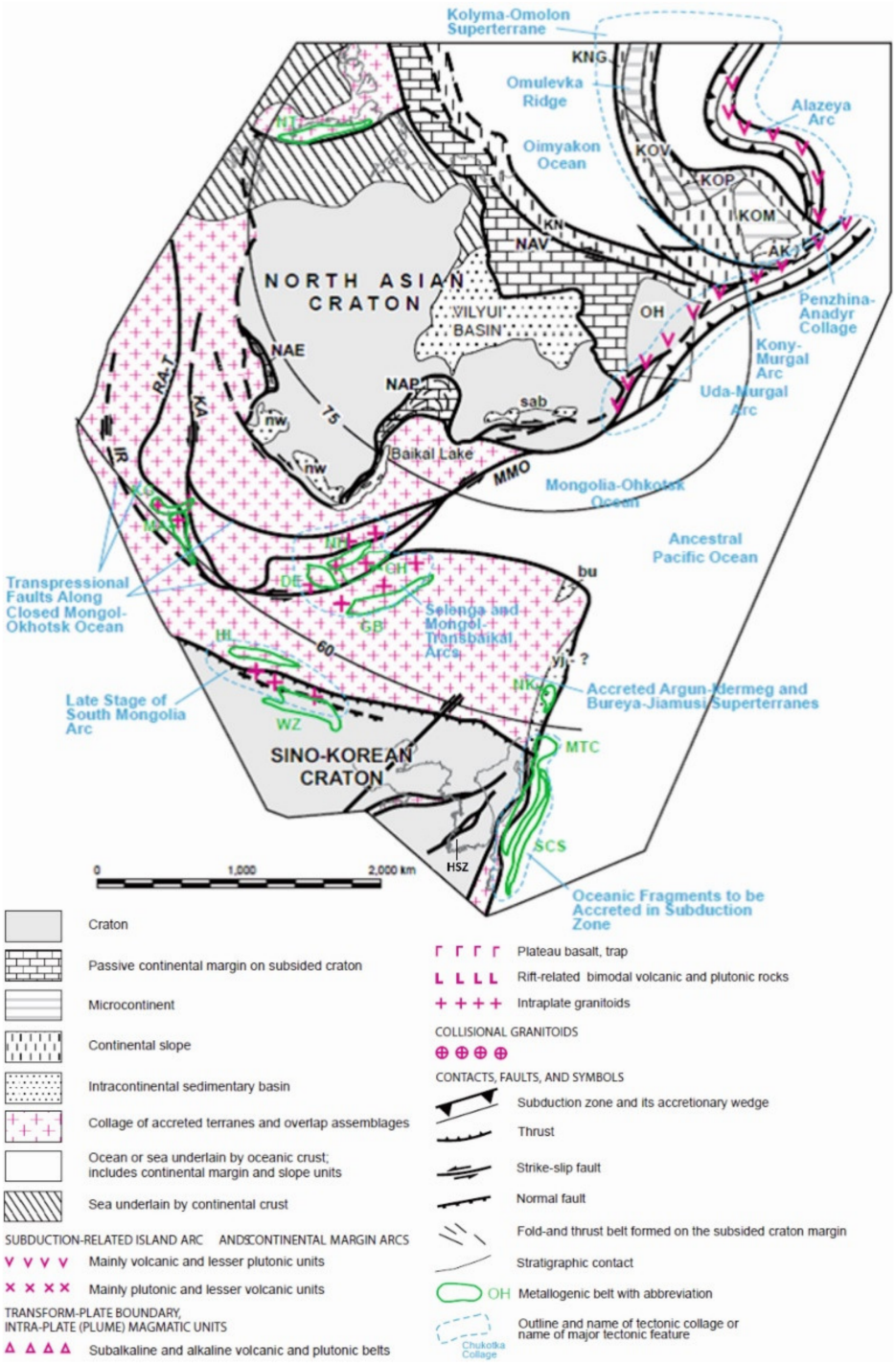

Figure 1. Paleotectonic reconstruction of NE Asia at 210 Ma, showing metallogenic belts of the Triassic–Early Jurassic (230–175 Ma) age [4]. North Asian Craton Margins: NAE—East Angara, NAP—Patom-Baikal; NAV—Verkhoyansk; Intracontinental sedimentary basins: bu—Bureya, nw—Western Siberia, sab—South Aldan, yj—Yanji-Jixi-Raohe; Terranes: AK—Avekov, KN—Kular-Nera, KNG—Nagondzha, KOM—Kolyma-Omolon, KOP—Prikolyma, KOV—Omulevka, OH—Okhotsk, HSZ—Honam Shear Zone; Strike-slip Faults and shear zones: IR—Irtysh, KA—Kuznetsk-Altai, MMO—Main Mongol-Okhotsk, RA-T—Rudny Altai-Taimyr; METALLOGENIC BELTS (green): CH—Central Hentii, DE—Delgerhaan, GB—Govi-Ugtaal-Baruun-Urt, HL—Harmorit-Hanbogd-Lugiingol, KG—Kalgutinsk, MTC—Mino-Tamba-Chugoku, MA—Mongol Altai, NH—North Hentii, NK—North Kitakami, NT—North Taimyr, SCS—Sambagawa-Chichibu-Shimanto, WZ—Wulashan-Zhangbei.

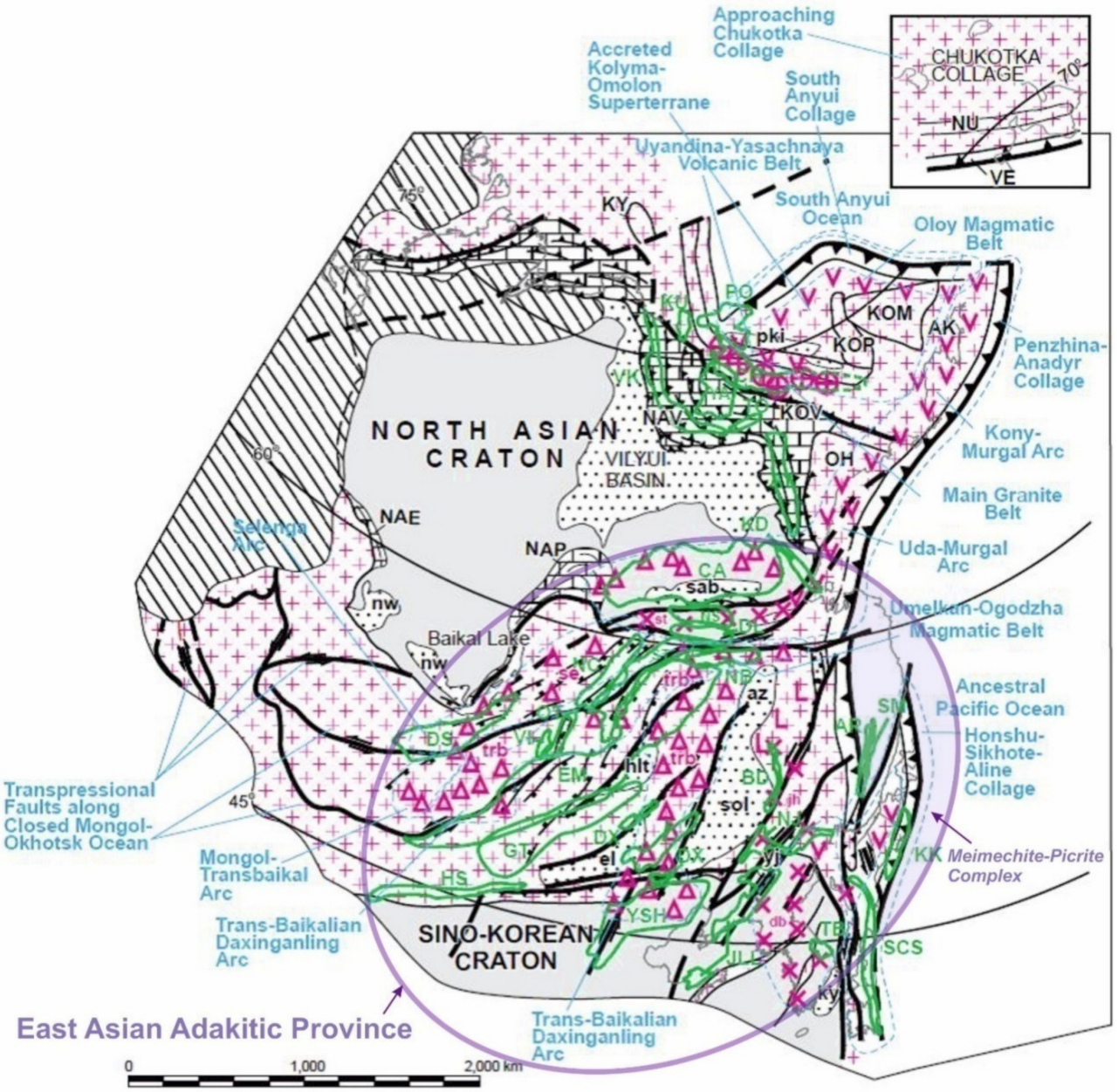

Figure 2. Paleotectonic reconstruction of NE Asia at 145 Ma, showing metallogenic belts of the Middle Jurassic–Early Cretaceous (175–96 Ma) age [4]. East Asian Adakitic Province is shown after [2]. The distribution of meimechite–picrite complex is suggested basing on the studies by [8–11]. North Asian Craton Margins: NAE—East Angara, NAP—Patom-Baikal; NAV—Verkhoyansk; Intracontinental sedimentary basins: el—Erlian, hlt—Hailar-Tamsag, ky—Kyongsang, nw—Western Siberia, pki-Ilin'-Tas, sab—South Aldan, sol—Songliao; Terranes: AK—Avekov, KY—Kotel'nyi, KOM—Kolyma-Omolon, KOP—Prikolyma, KOV—Omulevka, NU—Nutesyn, OH—Okhotsk, VE—Velmay; Active continental margins and granite belts: db—Daebo, jh—Jihei, se—Selenga, st—Stanovoy, trb—Trans-Baikalian-Daxinganling; METALLOGENIC BELTS: AR—Ariadny, AY—Allakh-Yun', BD—Bindong, CA—Chara-Aldan, CH—Chybagalakh, DL—Djeltulaksky, DS—Dzid-Selenginskiy, DX—Daxinganling, EM—East Mongolian-Priargunskiy-Deerbugan, GT—Govi-Tamsag, HS—Hartolgoi-Sulinheer, JLL—Jiliaolu, KD—Kondyor-Feklistov, KK—Kitakami, KU—Kular, NB—North Bureya, NC—Nerchinsky, NJ—North Jilin, NS—North Stanovoy, OT—Onon-Turinskiy, PO—Polousny, SM—Samarka, ST—Shilkinsko-Tukuringrskiy, TB—Taebaegsan, TO—Tompo, VI—Verkhne-Ingodinsky, VK—Verkhoyansk, YA-Yana-Adycha, SCS—Sambagawa-Chichibu-Shimanto. Other symbols are in Figure 1.

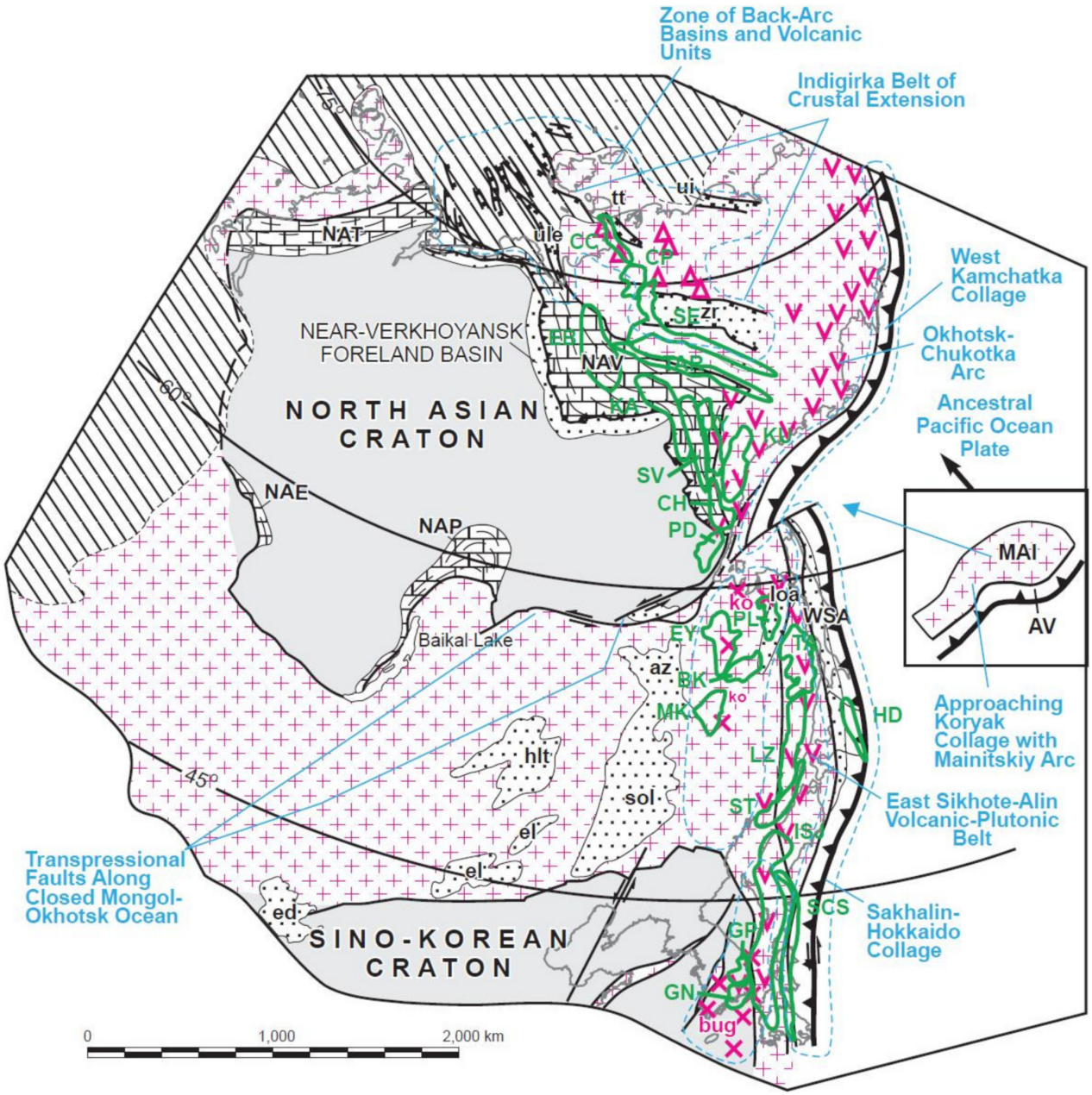

Figure 3. Paleotectonic reconstruction of NE Asia at 87 Ma, showing metallogenic belts of the Late Cretaceous–Paleogene (96–24 Ma) age [4]. North Asian Craton Margins: NAE—East Angara, NAP—Patom-Baikal, NAT—South-Taimyr, NAV—Verkhoyansk; Intracontinental sedimentary basins: az—Amur-Zeya, ed—Erduosi, el—Erlian, hlt—Hailar-Tamsag, loa—Lower Amur, sol—Songliao, tt—Tastakh, ui—Ust Indigirka, ule—Ust Lena, zr—Zyryanka; Terranes: AV—Alkatvaam, MAI—Mainitskiy, WSA—West Sakhalin; Active continental margins and granite belts: ko—Khingan-Okhotsk, bug—Bulgugsa; METALLOGENIC BELTS: BK—Badzhal-Komsomolsk, CC—Chokhchur-Chekurdakh, CH—Chelasin, CP—Central Polousny, EB—Eckyuchu-Billyakh, EY—Ezop-Yam-Alin, GN—Gyeongnam, GP—Gyeongpuk, HD—Hidaka, ISJ—Inner Zone Southwest Japan, KA—Khandyga, KU—Kukhtuy-Uliya, LZ—Luzhkinsky, MK—Malo-Khingan, PD—Preddzhugdzhursky, PL—Pilda-Limuri, SCS—Sambagawa-Chichibu-Shimantomk, SE—Selennyakh, ST—Sergeevka-Taukha, SV—South Verkhoyansk, TA—Tumnin-Anyuy, TAR—Taryn, UY—Upper Uydoma. Other symbols are in Figure 1.

3. Results and Discussion

In the proposed hypothesis [2], CTGE should be expressed in a distinct burst of endogenous activity and associated ore deposits. Figures 1–3 showing the temporal and spatial distribution of metallogenic belts and mineral deposits confirm this suggestion. The geodynamic classification of the deposits in this study was completely adopted from the database-compilers [3,4]. We only combined the plume- and transform plate-related belts and deposits into one geodynamic category, since the transform plate-related belts and deposits are considered doubtful, as is discussed below, in Section 3.1.

The Middle Jurassic–Early Cretaceous epoch was evidently richer in magmatic and metallogenic activities than the previous and following periods. Figure 4 quantitatively supports this distribution.

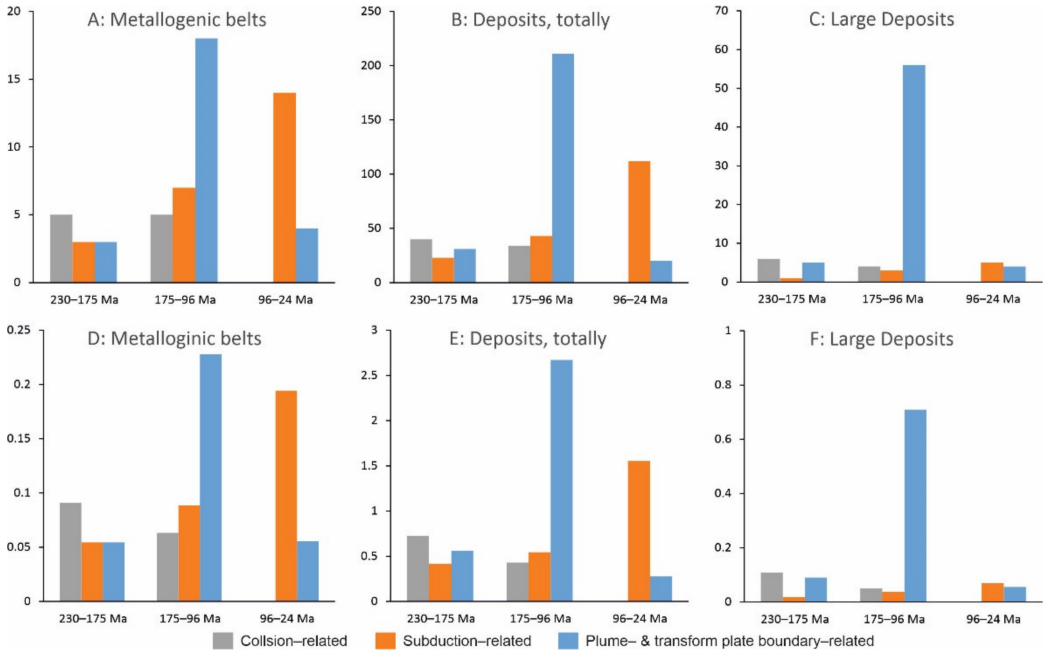

Figure 4. Age distribution of metallogenic belts and mineral deposits of NE Asia based on the data from [3,4]: (**A**–**C**)—total numbers, (**D**–**F**)—total number vs. duration of the corresponding metallogenic epoch (in million years).

Indeed, the time span including CTGE is distinguished by an anomalously high amount of mineral deposits, including the large ones. The deposits formed in the settings of transform plate boundaries and mantle plumes, as classified by [3,4], are especially numerous in this epoch (211 totally, including 56 of large size; Figure 4B,E). In contrast, the following Late Cretaceous–Paleogene epoch is predominantly subduction-related deposits, among which large deposits are very rare. Many of these deposits are associated with multi-stage magmatic complexes that began to form in the previous CTGE-related epoch.

3.1. Plume-Subduction Interaction during CTGE

Our data-sourcing reviews [3,4] attributed most metallogenic and magmatic belts of the Middle Jurassic–Early Cretaceous age to transform-plate boundaries and mantle plumes (Figures 2 and 4), among which the former absolutely predominate. The rare plume-related settings are associated with intra-plate magmatism. However, the abundant transform-plate boundaries are doubtful settings for magmatism because of the following reasons:

- The paleo-reconstruction of Figure 2 does not show any significant transform plate boundary, although strike-slip faults that transect the Eurasian plate including the Sino-Korean Craton are abundant;

- Magmatism in any form is less common along major strike-slip faults including transform plate boundaries [12], whereas it is widespread, forming numerous magmatic units in the Middle Jurassic–Early Cretaceous East Asia (Figure 2).

The review [2] presented an original geodynamic model for the widespread and heterogeneous magmatic, tectonic, and metallogenic activity in the Jurassic–Early Cretaceous East Asia assemblages. The model suggests a superplume arrived below an oceanic slab, flattening its subduction profile under the East Asian continental margin for tens of millions of years in the Jurassic and especially during the Early-Middle Cretaceous. Numerous slab windows developed via lateral extension above the plume, which could provide heat flows ascending through the slab, thus generating magmatic intrusions and fluid flows. A combination of partial melts in the upper slab, a thinned mantle wedge, and thickened lower crust, produced a complex suite of arc-type adakites, normal subduction-related rocks (volcanics and granites), and continental-type adakites accordingly [13–19]. Some plume-related complexes of East Russia, Japan, Northeast China, and Mongolia [8–11,20] also formed a part of this suite. The more recent tectonic and petrological studies [21–23] strongly confirmed this suggestion. The East-Asian Adakitic Province in Figure 2 shows a surficial projection of the plume-flat subduction interaction that provided the anomalous endogenous and metallogenic activities in the region during CTGE.

The mantle superplume considered above is of regional extent and, therefore, cannot alone justify the global/galactic attribution of the CTGE model. However, it may be correlated with many other plumes from different parts of the world. They are indicated by the following LIPs: Madagscar (90 Ma), Broken Ridge (95 Ma), Wallaby Plateau (96 Ma), Hess Rise (99 Ma), Central Kerguelen (100 Ma), Agulhas Plateau (100 Ma), Nauru (111 Ma), Southern Kerguelen (114 Ma), Rajmahal-Sylhet Traps (118 Ma), Whitsunday (120 Ma), Ontong Java (121 Ma), Manihiki Plateau (123 Ma), Maud Rise (125 Ma), High Arctic (Alfa Ridge) (130 Ma), Bunbury Basalts (132 Ma), Comei (132 Ma), Parana-Etendeka (132 Ma), Gascoyne (136 Ma), Magellan Rise (145 Ma), Shatsky Rise (147 Ma), Argo Margin (155 Ma), and NW Australia (160 Ma) [24]. Note that eight of them occurred at 120–132 Ma, the time of the suggested cosmic event responsible for CTGE.

3.2. Characteristic Ore Deposits

According to the geodynamic model described above, major endogenous activity in NE Asia during CTGE was expressed by magmatic units related to the mantle plume and flat subduction—mafic-ultramafic and adakitic complexes, respectively. Short descriptions of some mineral deposits, that are related to these magmatic complexes and, thus, characterize the CTGE metallogenic epoch, are presented below. The deposits are located in the Russian Far East, the geology of which is familiar to the authors of this study.

3.2.1. Mafic-Ultramafic Related Deposits, Ariadny Metallogenic Belt, Russian Far East

Magmatic bodies and related ores of the Ariadny belt are hosted by the Samarka accretionary wedge including fragments of Paleozoic ophiolitic rocks and greenstone, Carboniferous–Early Permian limestone, Middle Triassic chert, and Triassic–Jurassic clastic rocks (Figure 5). In some places, they are associated with meimechite and picrite flows occuring among the Jurassic shales. The ultramafic volcanic rocks of the meimechite-picrite complex bear some microscopic diamonds [25] and probably source fine-crystalline diamonds (carbonado) up to 8 mm in size into the local placer deposits [10] (Figure 5). Intrusive members of the complex commonly occur as small (2–15 km^2) elongated bodies differentiated from dunite (in cores) through wehrlite to clinopyroxenite and gabbro that sometimes are cut by syenite and carbonatite [26]. They are hosted by shales and cherts and intruded by the explosive picrite pipes. Gabbro and pyroxenite include iron-titanium deposits with gold and platinum mineralization, while alkaline rocks (syenites) contain REE mineralization. Rich ilmenite placers with commercial contents of gold and platinum accompany the massifs. Larger elongated (up to 15 km) massifs are hosted by volcanic

and siliceous bedrocks. They are less differentiated and consist of wehrlite-dunite lenses intruded by numerous veins of pegmatitic clinopyroxenite.

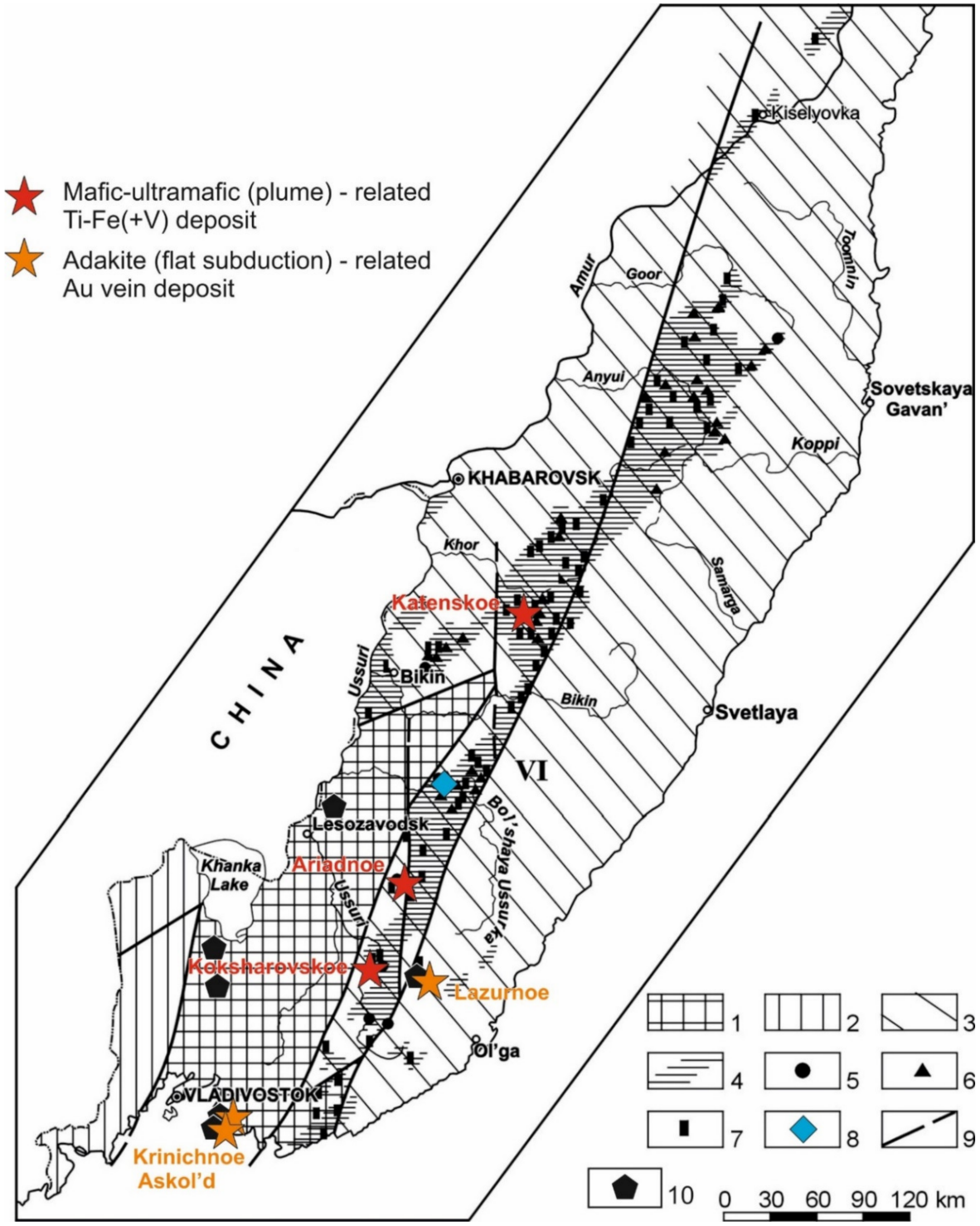

Figure 5. Location of the Jurassic–Early Cretaceous meymechite-picrite and Early Cretaceous adakite complexes and related mineral deposits in the Russian Far East (after [10,26] with additions from [18]). 1—Khanka crystalline massif; 2—Late Paleozoic (Laoelin-Grodekov) fold belt; 3—Mesozoic (Sikhote-Alin) fold belt; 4—volcanic area of the Jurassic–Early Cretaceous accretionary wedge; 5–7—alkali-ultrabasic complex: 5—diatreme, 6—meymechite subvolcanic body; 7—dunite-pyroxenite intrusion; 8—diamond occurrence in the gold placer; 9—general fault; 10—small intrusions of the Early Cretaceous adakitic rocks.

The detailed mineralogical, isotopic (Nd, Sr, C, O) and geochemical petrological studies [8,10,23,25–30] clearly identified a deep enriched mantle source of the meimechite-picrite rocks (Figure 6) that is close to the source of the kimberlitic melts. The kimberlitic affinity is especially well manifested by the mineral suite including diamond, picroilmenite, and Ti-rich Cr-spinel (Figure 7).

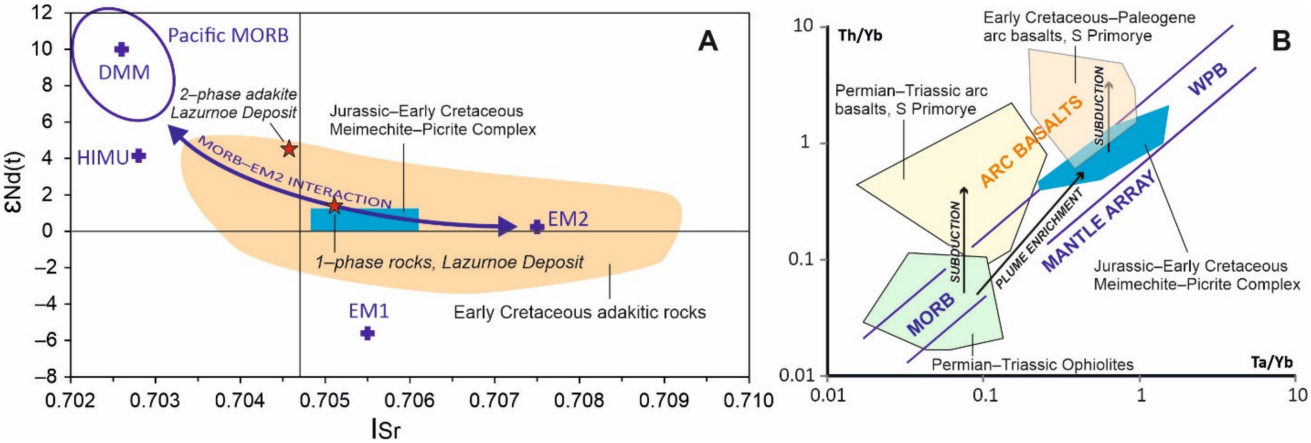

Figure 6. Isotopic-geochemical evidence of interaction between mantle plume and subduction in the Sea-of-Japan region (simplified from [23]). (**A**) Sr-Nd isotopic compositions of the Jurassic–Early Cretaceous mafic-ultramafic and adakitic rocks (after [18]) with addition from [31] for rocks of the Lazurnoe porphyry Cu-Mo (+Au, Ag) deposit. (**B**) Th/Yb versus Ta/Yb (after [32]) in the late Paleozoic–Early Cenozoic mafic rocks. The MORB, Mid-Ocean Ridge Basalt; DMM, Depleted Mantle Member; WPB, Within-Plate Basalt; HIMU, EM1, and EM2, enriched mantle sources [33].

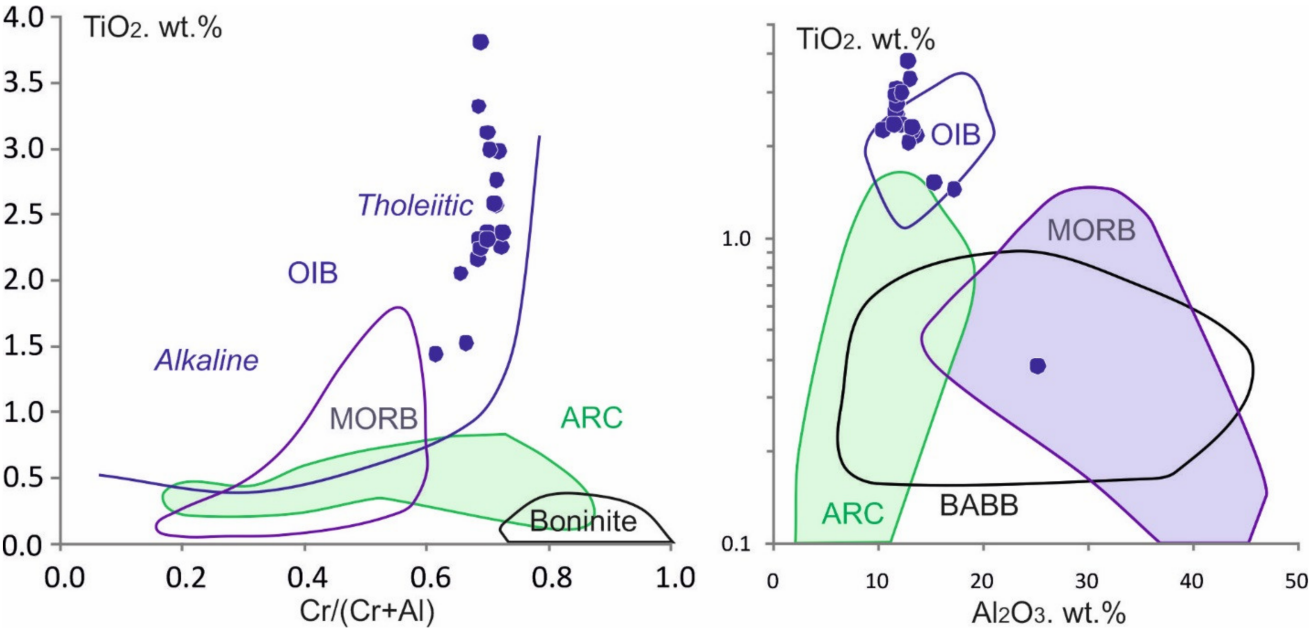

Figure 7. TiO_2 vs. Cr/(Cr + Al) and Al_2O_3 diagrams by [34,35], respectively, for Cr-spinel from the meimechite-picrite complex of Sikhote-Alin (simplified from [23]). MORB, Mid-Ocean Ridge Basalt; OIB, Oceanic Island Basalt; ARC, Arc (subduction-related) basalts; BABB, Back-Arc Basin basalt.

The Ariadny metallogenic belt is represented by three large deposits, namely the Katenskoe, Ariadnoe, and Koksharovskoe deposits (Figure 5).

The Koksharovskoe Ti-Fe(+V)-P deposit is the best studied (Figure 8) [29,36–38]. It consists of disseminated ilmenite, Ti-magnetite, titanite, and apatite that occur in the syenite (carbonatite)-pyroxenite ring bodies with U-Pb zircon ages of 149–161 and 96–98 Ma

(samples 26, 28, and 32 from http://geochron-atlas.vsegei.ru/, in Russian, accessed on 23 March 2022). Two Ti-Fe(+V) ore types are distinguished: (1) Mg-rich (up to 7.6 wt% MgO) ilmenite associated with primary magmatic pyroxenite from the intrusion cores; and (2) titanite–ilmenite–magnetite suite in the altered biotite-bearing pyroxenite [38]. Vanadium is abundant in Ti-rich magnetite, while REE and Ta are associated with titanite. Minor PGE minerals also occur in association with Cr spinel and ilmenite. Some intrusive rocks are weathered, including economic concentrations of vermiculite. The average ore grades are 1 to 10% P_2O_5, and 3.3 to 4.5 % TiO_2 [3].

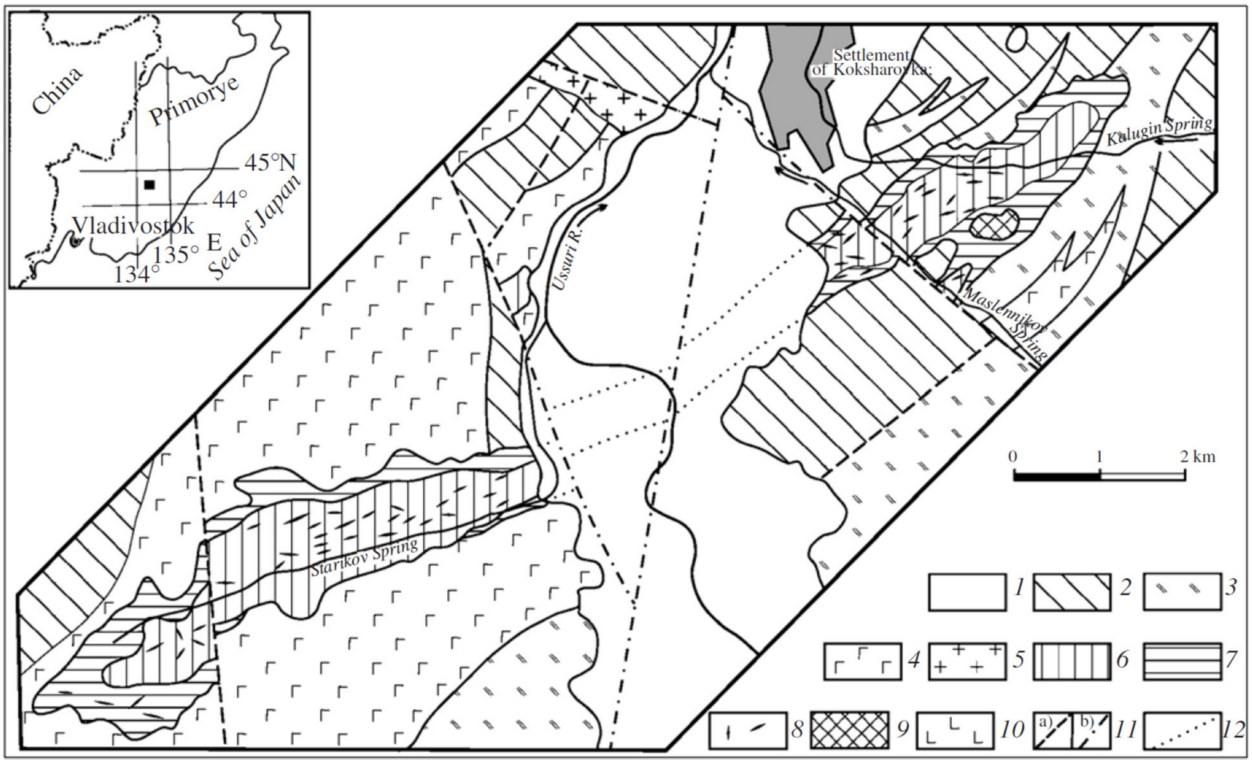

Figure 8. Geological map of the Koksharovka alkaline ultrabasic massif (after [29,36,38]). (1) Stream sediments; (2–4) Triassic Jurassic siliceous–terrigenous–volcanic rock complex (matrix of the accretionary wedge) with lenses and beds of siliceous (3) and volcanic (4) rocks: basalt lavas and tuffs; (5) Late Cretaceous granite; (6–9), alkaline ultrabasic complex: biotite-bearing pyroxenite (6), amphibole-bearing pyroxenite (7), syenite dike (8) and carbonatite (9); (10) diabase and gabbro-diabase; (11) proven (a) and supposed (b) faults; (12) contours of the pyroxenite body beneath the alluvial deposits inferred from geophysical data.

The AriadnoeTi-Fe(+V) deposit [39] also consists of abundant disseminated ilmenite that occurs in layers of pyroxene-hornblende gabbro and pyroxenite in layered intrusions. The ilmenite-bearing layers are several tens of meters thick and several hundred meters long. The K-Ar data of coexisting kaersutite and Ti-biotite from the latest picrite pipes and from the ring intrusion show a short age interval of 159–152 Ma. Ilmenite contains rare PGE inclusions. The average ore grades are 1.0 to 11.8% TiO_2 and 0.086% V_2O_5 [3].

The KatenskoeTi-Fe(+V)-Cr-PGE deposit [37] consists of disseminated ilmenite in Early Cretaceous pyroxene-hornblende gabbro and olivine gabbro. The deposit consists of lenticular bodies that are several tens of meters thick and at least 1 km long.

Generally, the meimechite-picrite complex and associated ores represent a rare, probably unique phenomenon of superplume-related melts and fluids injected into an accretionary wedge, which, at the time of injection, was under formation conditions.

3.2.2. Adakite-Related Deposits, Seregeevka-Taukha and Luzhkinsky Metallogenic Belts, Russian Far East

In contrast to the mafic-ultramafic-related deposits, the adakite-related Au-veins and porphyry Cu-Mo (+Au, Ag) ores of Sikhote-Alin formed in the post-accretionary circumstances. Sodov et al. [3], based mainly on the K-Ar dates, attributed them to the Sergeevka-Taukha and Luzhkinskymetallogenic belts of the Late Cretaceous (96–72 Ma) age (Figure 3). However, the more recent U-Pb zircon dating of the Krinichnoe (Sergeevka-Taukha belt) and Lazurnoe (Luzhkinsky belt) deposits allows reconsideration of this definition. The ore-related adakites of the former showed 131.4 ± 1.5 Ma [18], while the latter was 103.5 ± 1.5 Ma [31], indicating the previous CTGE-associated metallogenic epoch, although a later alteration of the major ores is highly probable.

The Jurassic–Early Cretaceous ore-related adakitic rocks of Sikhote-Alin are well described in the literature [18] and references therein. They are typical arc adakites, derived from subducted slab melts in contrast to continental-type adakites that are widely distributed in the intracontinental parts of East Asia and derived from the lower crustal melts [14–18,40].

The Askol'd Au-vein deposit is located at the Askol'd Island in Peter-the-Great Bay, northwestern Japan Sea (Figures 5 and 9). It is associated with the intrusive complex represented by two stock-like bodies of biotite-hornblende granitoids named the Central and Western intrusions [41]. They are located in the middle and northwestern parts of the island, respectively. Both intrusions are composed of medium-grained biotite-hornblende adakitic granitoids with numerous inclusions of fine-grained diorite ranging from 5 to 20 cm in size. The age of adakites, according to the results of Rb-Sr isotopic dating is 104 Ma, and the K-Ar biotite date is about 98 Ma [42,43]. Both large intrusive bodies are accompanied by numerous dikes and veins consisting of granite-aplites, pegmatites, quartz, granite-porphyries, dacitic, andesite-dacitic, and diabase porphyrites. Their thickness varies from 0.1 to several tens of meters, whereas the length is up to 300 m. The ores are confined to the eastern contact of the Central massif, which contains numerous apophyses. They are represented by an Au-quartz vein stockwork in the granitoids that are altered into greisen. The deposit is prospected to depths of more than 100 m. It is medium in size, with Au grades of 5.9 to 7.6 g/t Au [3]. The lode ores are associated with on-land and off-shore gold placers.

The Krinichnoe Au (+Ag)-vein deposit is located on land, 13 km to NNE of the Askol'd deposit [43,44]. Geology of the two deposits is similar. The Krinichnoe lode deposit consists of gold–pyrite–quartz and quartz-carbonate zones in the adakitic granitoid pluton that intrudes metamorphosed Paleozoic volcanic and sedimentary rock. Sulfide-poor gold–pyrite–quartz ores occur in bodies of variable shape and size. They contain up to 2.8 g/t Au and up to 171 g/t Ag [3].

The Lazurnoe porphyry Cu-Mo (+Au, Ag) deposit is associated with an asymmetric intrusive massif hosted by the Early Cretaceous turbidites [3,31]. The massif consists of two bodies, namely the North and South Stocks that were formed one after another (Figure 10). The early phase (North Stock) has a K-Ar hornblende age of 110 ± 4 Ma. It is represented by monzo-gabbro-diorites, which geochemistry indicate the crustal contamination and following magmatic differentiation (appearance of more felsic rocks, δ^{18}Osmow = 8.3‰ in plagioclase, $^{176}Hf/^{177}Hf$ = 0.2822227 − 0.2826510 in zircon, $^{143}Nd/^{144}Nd$ = 0.512579 ± 5 and $^{87}Sr/^{86}Sr$ = 0.705155 ± 14; Figure 6; [31]). The second phase (South Stock) with the U-Pb zircon age of 103.5 ± 1.5 Ma (SHRIMP) consists of adakitic monzodiorite with no signs of crustal contamination. It represents a more primitive magma based on its trace-element (Figure 11) and isotopic compositions (δ^{18}Osmow = 5.9‰ in hornblende, $^{176}Hf/^{177}Hf$ = 0.2828270 − 0.2831770 in zircon, $^{143}Nd/^{144}Nd$ = 0.512733 ± 3 and $^{87}Sr/^{86}Sr$ = 0.704569 ± 12; Figure 6) [31].

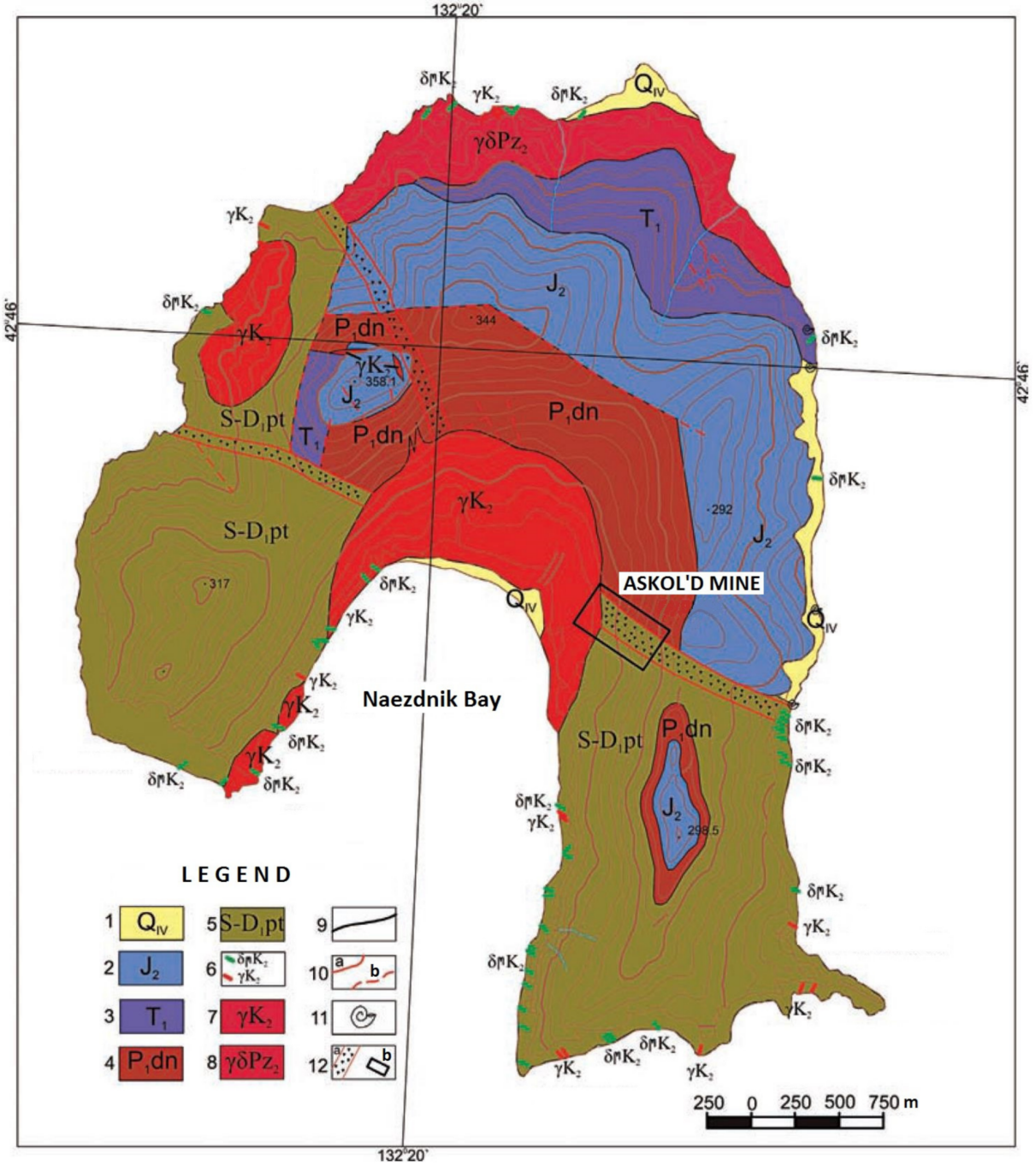

Figure 9. Geological map of the Askol'd Island (after [41]). 1—soft sediments; 2—Middle Jurassic sandstones and mudstones; 3—Lower Triassic conglomerates and sandstones; 4—Lower Permian quartz porphyry; 5—Silurian–Devonian metamorphosed conglomerates, biotite hornfelses, and meta-effusives; 6—Cretaceous dikes of diorite (δμK2), granite and aplite veins (γK2); 7—Cretaceous biotite-hornblende adakiticgranitoides and plagiogranites; 8—Middle Paleozoic granodiorites, diorites, gabbro-diorites; 9—geological boundaries; 10—faults proven (a) and supposed (b); 11—findings of fossil fauna; 12—ore-bearing tectonic zones (a) and the site of old mines (b).

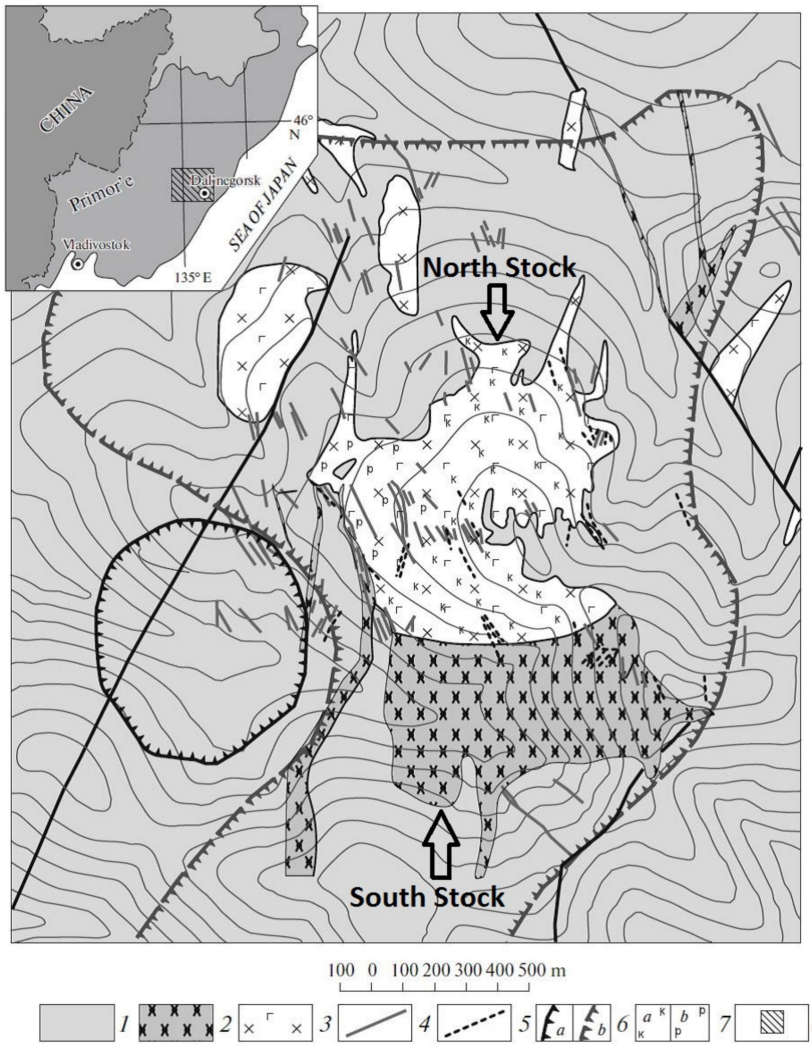

Figure 10. A geologic scheme of the Lazurnoe deposit (after [31] and references therein). (1) Early Cretaceous sedimentary rocks; (2) adakitic monzodiorite and monzo-gabbro-diorite (2nd phase); (3) gabbro–monzodiorite and diorite (1st phase); (4) dykes of quartz monzodiorite; (5) quartz–sulfide veins and porphyry sulfide ores; (6) projections to the surface of: (a) the hidden porphyritic massif, (b) the copper–porphyry mineralization; (7) hydrothermal alterations: (a) potassium-feldspar, (b) propylitic; (8) the study area.

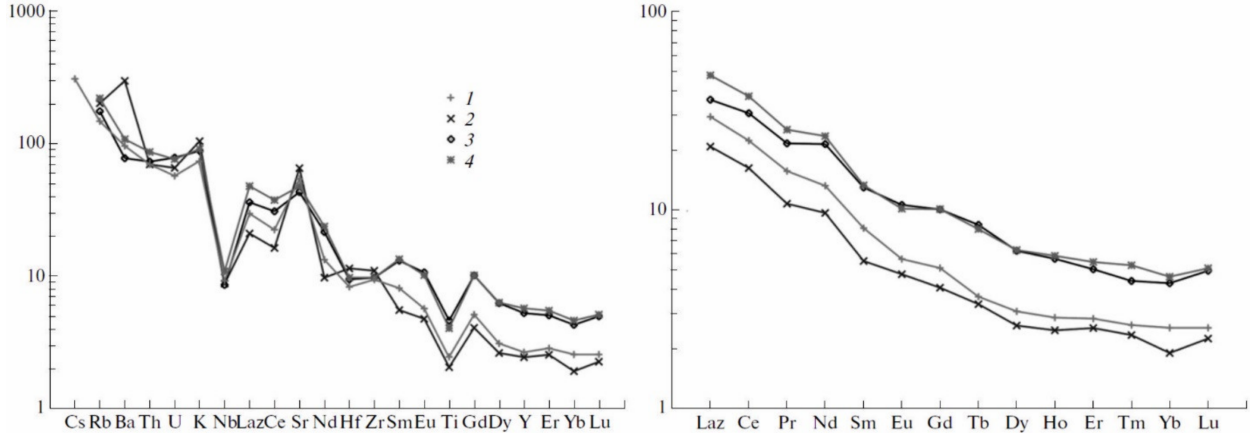

Figure 11. Multicomponent diagrams for magmatic rocks of the Lazurnoe deposit, normalized to the primitive mantle (after [31]). 1 and 2—adakitic monzodiorites from the South Stock; 3 and 4—gabbro-monzodiorites from the North Stock.

Ores of Lazurnoe deposit contain up to 3 g/t Au, 0.3–0.6% Cu, 0.008–0.2% Mo. They are concentrated in and around the North Stock in the form of numerous carbonate–sulfide veins and disseminated sulfide grains (Figure 10). The chalcopyrite-bornite-pyrite-sphalerite-molybdenite mineralization is traced to a depth of 300 m. The sulfides are associated with propylitic (epidote, chlorite, sericite, and carbonate) and potassium-feldspar (K-feldspar, biotite, sericite, chlorite, magnetite, sulfides) alterations (Figure 10). Quartz-carbonate veins with sulfides occur near the surface. The isotopic composition of sulfur ($\delta^{34}S$ = +0.3–+0.62) from pyrite and chalcopyrite indicates a magmatic origin of the ores. The isotopic composition of oxygen ($\delta^{18}Osmow$ = 7.2‰) in plagioclase, which is hosted by the altered rocks, is evidence for fluid–mantle equilibrium. The ore-related alteration of the first phase rocks including high-temperature biotite alteration is attributed to the second phase melts, which were saturated with fluids. This conclusion is supported by the K-Ar age of secondary biotite in monzo-gabbro-diorite (101 ± 2.5 Ma) from the North Stock that coincides with the age of the second phase magmatic rocks of the South Stock [31].

Further detailed studies of Mesozoic geological events are available for comparative considerations in relation to "Turn of the Cretaceous" sequences, magmatic episodes, and mineralization, within Mesozoic tectonic settings elsewhere. These include examples both in the NE Asian active margins region to the north [45] and to the eastern paleo-margin of China [46,47]. The study in the NE Asian active margin in the Verkhoyansk–Kolyma orogenic belt revealed a dramatic change in the Late Cretaceous sediments of syn-depositional detrital zircons of 88–90 Ma age. They were derived from the volcanic lavas, volcaniclastics and granitoid plutons of the Okhotsk–Chukotka magmatic belt that ended its activity at 86–87 Ma [45]. The study of Early Cretaceous granitic plutons and their enclaves in the eastern margin to the Chinese Craton indicated a coeval formation within error at 116–118 Ma and were generated within a partial melting episode during the peak of underlying lithospheric thinning [46]. The specific Cretaceous endogenous processes resulted in the extensive and diverse group of mineral deposits formed from 145 to 70 Ma along the eastern Asian continental margin from northern Vietnam, through eastern China, Korea, Japan, and to Far East Russia, representing a good example of a regional extension-related metallogenic province [47]. The authors of the mentioned studies [42–44] do not necessarily share our "galactic" view on the Cretaceous evolution, although their ideas seem close to our ideas, at least, do not contradict them.

4. Conclusions on the CTGE-Related Metallogeny

As predicted by the CTGE hypothesis, the Triassic–Early Jurassic geodynamic activity in NE Asia was simple, producing a relatively small amount of metallogenic belts and mineral deposits related to active and passive continental margins and undeveloped (incipient, granitic) intraplate magmatism (Figure 1). In contrast, the enormous geodynamic activity around CTGE initiated the Jurassic–Early Cretaceous superplume. The related melts and fluids injected into an accretionary wedge, when both plume and accretion were actively developed. At that time, subduction of the Pacific plate was flattened by the superplume under the former eastern Eurasia (Figure 2). This resulted in many metallogenic belts and mineral deposits that were numerous in amount, large in size, and diverse in composition. The characteristic ores are represented by the unique plume-related Ti-Fe-V + P + Cr-PGE + Au + diamond deposits. Other characteristic representatives of the CTGE epoch are the porphyry Cu-Mo and Au (+Ag)-vein deposits, which formation, however, continued in the following Early–Late Cretaceous metallogenic epoch, probably reaching a maximum in the middle Cretaceous. These deposits were generated by the slab- and crust-derived adakitic and granitic melts, and fluids intruded into the tectonically consolidated Earth's crust under influence of the same superplume, but at the vanishing stage of its development. The Late Cretaceous–Paleogene epoch is indicated by a decreasing metallogenic activity in general, and an increasing role of subduction-related deposits in particular.

Supplementary Materials: The following supporting information can be downloaded at: https://www.mdpi.com/article/10.3390/min12040400/s1, Table S1: The metallogenic belts and lode deposits of NE Asia for the Triassic–Early Jurassic, Middle Jurassic–Early Cretaceous, and Early Cretaceous–Paleogene epochs (modified after [3]).

Author Contributions: V.P.N., Conceptualization, methodology, writing—original draft preparation; F.L.S., writing—review and editing; E.V.N., visualization. All authors have read and agreed to the published version of the manuscript.

Funding: This research received no external funding.

Data Availability Statement: The data supporting reported results can be found at the freely available USGS Web Site http://pubs.usgs.gov/of/2003/of03-220 (accessed on 23 March 2022) or using the DOI record https://doi.org/10.3133/ofr2003220.

Acknowledgments: The authors highly appreciate the discount of processing charge offered by MINERALS for this article. We also are grateful to the anonymous reviewers whose comments were used to significantly improve the paper.

Conflicts of Interest: The authors declare no conflict of interest.

References

1. Nechaev, V.P. On the galactic influence on the Earthduring the last seven hundred million years. *Bull. Far East. Branch Russ. Acad. Sci.* **2004**, *2*, 102–112. (In Russian). English Version. Available online: https://www.researchgate.net/profile/Victor_Nechaev (accessed on 23 March 2022).
2. Nechaev, V.P.; Dai, S.; Sutherland, F.L.; Graham, I.T.; Nechaeva, E.V. The Cretaceous turn of geological evolution: Key evidence from East Asia. *Acta Geol. Sin.* **2018**, *92*, 1991–2003. [CrossRef]
3. Sodov, A.; Biryul'kin, G.V.; Byamba, J.; Davydov, Y.V.; Dejidmaa, G.; Distanov, E.G.; Dorjgotov, D.; Gamyanin, G.N.; Gerel, O.; Fridovskiy, V.Y.; et al. *Significant Metalliferous and Selected Non-Metalliferous Lode Deposits, and Selected Placer Districts of Northeast Asia*; Nokleberg, W.J., Bounaeva, T.V., Miller, R.J., Seminskiy, Z.V., Diggles, M.F., Eds.; U.S. Geological Survey Open-File Report 03-220: 2003; Western Mineral Resources, U.S. Geological Survey: Reston, VA, USA, 2003. [CrossRef]
4. U.S. Geological Survey. *Metallogenesis and Tectonics of Northeast Asia*; Nokleberg, W.J., Ed.; U.S. Geological Survey Professional Paper 1765: 2010; U.S. Geological Survey: Reston, VA, USA, 2010; p. 624. Available online: https://pubs.usgs.gov/pp/1765 (accessed on 23 March 2022).
5. Weissman, P.R. The Solar System and Its Place in the Galaxy. In *Encyclopedia of the Solar System*, 3rd ed.; Spohn, T., Breuer, D., Johnson, T., Eds.; Elsevier: Amsterdam, The Netherlands, 2014; pp. 3–28. Available online: https://www.sciencedirect.com/book/9780124158450/encyclopedia-of-the-solar-system#book-description (accessed on 23 March 2022).
6. Castillo, P.R. An overview of adakite petrogenesis. *Chin. Sci. Bull.* **2006**, *51*, 257–268. [CrossRef]
7. Hernández-Uribe, D.; Hernández-Montenegro, J.D.; Cone, K.A.; Palin, R.M. Oceanic slab-top melting during subduction: Implications for trace element recycling and adakite petrogenesis. *Geology* **2020**, *48*, 216–220. [CrossRef]
8. Shcheka, S.A. Meymechite–picritic complexes of the Sikhote-Alin. *Dokl. Akad. Nauk. SSSR* **1977**, *234*, 444–447. (In Russian)
9. Ishiwatari, A.; Ichiyama, Y. Alaskan-type plutons and ultramafic lavas in Far East Russia, Northeast China, and Japan. *Int. Geol. Rev.* **2004**, *46*, 316–331. [CrossRef]
10. Shcheka, S.A.; Ignat'ev, A.V.; Nechaev, V.P.; Zvereva, V.P. First diamonds from placers in Primorie. *Petrology* **2006**, *14*, 299–317.
11. Ishiwatari, A.; Ichiyama, Y.; Ganbat, E. Plume type ophiolites in Japan, East Russia and Mongolia: Peculiarity of the Late Jurassic examples. The General Assembly of the European Geosciences Union, Vienna, Austria, 7–12 April 2013.
12. Duarte, J.C. (Ed.) *Transform Plate Boundaries and Fracture Zones*, 1st ed.; Elsevier: Amsterdam, The Netherlands, 2019; p. 478.
13. Davis, G.A. The Yanshan belt of North China: Tectonics, adakitic magmatism, and crustal evolution. *Earth Sci. Front.* **2003**, *10*, 373–384.
14. Liu, S.A.; Li, S.G.; He, Y.S.; Huang, F. Geochemical contrasts between early Cretaceous ore-bearing and ore-barren high-Mg adakites in central-eastern China: Implications for petrogenesis and Cu–Au mineralization. *Geochim. Et Cosmochim. Acta* **2010**, *74*, 7160–7178. [CrossRef]
15. Liu, S.; Li, S.; Guo, S.; Hou, Z.; He, Y. The Cretaceous adakitic–basaltic–granitic magma sequence on south-eastern margin of the North China Craton: Implications for lithospheric thinning mechanism. *Lithos* **2012**, *134–135*, 163–178. [CrossRef]
16. Ma, Q.; Zheng, J.P.; Xu, Y.G.; Griffin, W.L.; Zhang, R.S. Are continental "adakites" derived from thickened or foundered lower crust? *Earth Planet. Sci. Lett.* **2015**, *419*, 125–133. [CrossRef]
17. Chen, B.; Jahn, B.M.; Suzuki, K. Petrological and Nd–Sr–Os isotopic constraints on the origin of high-Mg adakitic rocks from the North China Craton: Tectonic implications. *Geology* **2013**, *41*, 91–94. [CrossRef]
18. Wu, J.T.J.; Jahn, B.M.; Nechaev, V.; Chashchin, A.; Popov, V.; Yokoyama, K.; Tsutsumi, Y. Geochemical characteristics and petrogenesis of adakites in Sikhote-Alin, Russian Far East. *J. Asian Earth Sci.* **2017**, *145*, 512–529. [CrossRef]

19. Osozawa, S.; Usuki, T.; Usuki, M.; Wakabayashi, J.; Jahn, B. Trace elemental and Sr-Nd-Hf isotopic compositions, and U-Pb ages for the Kitakami adakitic plutons: Insights into interactions with the early Cretaceous TRT triple junction offshore Japan. *J. Asian Earth Sci.* **2019**, *184*, 103968. [CrossRef]
20. Prikhod'ko, V.S.; Petukhova, L.L. Ultramafic dykes in the Samarka accretionary complex of Sikhote-Alin. In *Volcanism and Geodynamics*; Koroteev, V.A., Ed.; IGG UrO RAN: Ekaterinburg, Russia, 2011; pp. 152–154. (In Russian)
21. Golozubov, V.V.; Khanchuk, A.I. The Heilongjiang complex as a fragment of a Jurassic accretionary wedge in the tectonic windows of the overlying plate: A flat slab subduction model. *Russ. J. Pac. Geol.* **2021**, *15*, 279–292. [CrossRef]
22. Golozubov, V.V.; Simanenko, L.F. Tectonostratigraphy of the Jurassic accretionary prisms in the Sikhote-Alin region of Russian Far East. *Sci. Rep.* **2021**, *11*, 19337. [CrossRef]
23. Nechaev, V.P.; Sklyarov, E.V.; Isozaki, Y.; Kruk, N.N.; Travin, A.V.; Tsutsumi, Y.; Nechaeva, E.V. A major change in magma sources in late Mesozoic active margin of the circum-Sea of Japan domain: Geochemical constraints from late Paleozoic to Paleogene mafic dykes in the Sergeevka belt, southern Primorye, Russia. *Isl. Arc* **2021**, *30*, e12426. [CrossRef]
24. Torsvik, T.; Burke, K. Large igneous province locations and their connections with the core–mantle boundary. In *Volcanism and Global Environmental Change*; Schmidt, A., Fristad, K., Elkins-Tanton, L., Eds.; Cambridge University Press: Cambridge, UK, 2015; pp. 30–46. [CrossRef]
25. Ivanov, V.V.; Kolesova, L.G.; Khanchuk, A.I.; Akatkin, V.N.; Molchanova, G.B.; Nechaev, V.P. Find of diamond crystals in Jurassic rocks of the meymechite-picrite complexin the SikhoteAlin orogenic belt. *Dokl. Earth Sci.* **2005**, *404*, 975–978.
26. Shcheka, S.A.; Vrzhosek, A.A.; Vysotskiy, S.V. Jurassic meymechite–picrite complexes of Primorye, Russia: Comparative study with komatiite and Japanese picrite suites. In *Plumes and Problems of Deep Sources of Alkaline Magmatism*; Vladykin, N.V., Ed.; Publishing House of the Irkutsk State Technical University: Khabarovsk, Russia, 2003; pp. 184–200.
27. Shcheka, S.A. *Basite and Hyperbasite Intrusions and Inclusions in Effusives of Far East*; Nauka: Moscow, Russia, 1983; p. 165. (In Russian)
28. Esin, S.V.; Prikhod'ko, V.S.; Ponomarchuk, V.A.; Travin, A.; Palesskii, S.V. Petrogenesis of Mesozoic alkaline-picrite-melaleucite association in the central Sikhote Alin. *Russ. Geol. Geophys.* **1996**, *37*, 17–27. (In Russian)
29. Oktyabr'skii, R.A.; Vladykin, N.V.; Lennikov, A.M.; Vrzhosek, A.A.; Yasnygina, T.A.; Rasskazov, S.V.; Moskalenko, E.Y.; Velivetskaya, T.A. Chemical composition and geochemical characteristics of the Koksharovka alkaline ultrabasic massif with carbonatites, Primorye. *Geochem. Int.* **2010**, *48*, 778–791. [CrossRef]
30. Simonov, V.A.; Prikhodko, V.S.; Kovyazin, S.V.; Kotlyarov, A.V. Petrogenesis of meymechites of SikhoteAlin inferred from melt inclusions. *Russ. J. Pac. Geol.* **2014**, *8*, 423–442. [CrossRef]
31. Sakhno, V.; Kovalenko, S.; Alenicheva, A. Monzonitoid magmatism of the copper porphyritic Lazurnoe deposit (South Primor'e): U-Pb and K-Ar geochronology and peculiarities of ore-bearing magma genesis by the data of isotopic-geochemical studies. *Dokl. Earth Sci.* **2011**, *438*, 569–577. [CrossRef]
32. Pearce, J.A. Role of sub-continental lithosphere in magma genesis at active continental margins. In *Continental Basalts and Mantle Xenoliths*; Hawkesworth, C.J., Nurry, M.L., Eds.; Shiva: Cheshire, UK, 1983; pp. 230–249.
33. Hart, S.R. Heterogeneous mantle domains: Signatures, genesis and mixing chronologies. *Earth Planet. Sci. Lett.* **1988**, *90*, 273–296. [CrossRef]
34. Arai, S. Chemistry of chromian spinel in volcanic rocks as a potential guide to magma chemistry. *Mineral. Mag.* **1992**, *56*, 173–184. [CrossRef]
35. Lenaz, D.; Princivalle, F. Crystal chemistry of detrital Cr-spinels from SE Alps and Outer Dinarides: A new tool to discriminate supplies from different provenance areas with similar tectonic setting? *Can. Mineral.* **2005**, *43*, 1305–1314. [CrossRef]
36. Zalishchak, B.L. *Koksharovskii Massif of the Ultrabasic and Alkaline Rocks (Southern Primorye)*; Nauka: Moscow, Russia, 1969; p. 115. (In Russian)
37. Shcheka, S.A.; Vrzhosek, A.A.; Bratchuk, O.N. Minerals and forms for iron-titanium deposits of the Sikhote-Alin Area. In *Abstracts for Conference on Ore Deposits of the Far East*; U.S.S.R. Academy of Sciences, Far East Geological Institute: Vladivostok, Russia, 1991; pp. 103–105. (In Russian)
38. Rub, M.G.; Rub, A.K.; Chistyakova, N.I.; Rub, I.A.; Krivoschekov, N.N. Ultrabasic alkaline rocks of the Koksharovskii massif (Primorye) as potential titanium source. *Tikhookeanskaya Geol.* **1995**, *14*, 21–36. (In Russian)
39. Shcheka, S.A.; Vrzhosek, A.A. A rare-type igneous platinum-gold mineralization in mafic-ultramafic intrusives. In *Typomorphous Assemblages of Accessory Minerals and Microelements*; Shcheka, S.A., Ed.; U.S.S.R. Academy of Sciences, Far East Geological Institute: Vladivostok, Russia, 1985; pp. 82–92. (In Russian)
40. Wang, Q.; Xu, J.F.; Zhao, Z.H.; Bao, Z.W.; Xu, W.; Xiong, X.L. Cretaceous high potassium intrusive rocks in the Yueshan-Hongzhen area of east China: Adakites in an extensional tectonic regime within a continent. *Geochem. J.* **2004**, *38*, 417–434. [CrossRef]
41. Lelikov, E.P. The Askold Island: Geological structure and gold-bearing. *Bull. Far East. Branch Russ. Acad. Sci.* **2013**, *6*, 198–204. (In Russian)
42. Gonevchuk, V.G.; Gonevchuk, G.A.; Sayadyan, G.R.; Seltman, R. Rare earth elements in tin-bearing and gold-bearing granitoids of Sikhote-Alin as indicators of their genesis. In *Geodynamics and Metallogeny*; Khanchuk, A.I., Ed.; Dal'nauka: Vladivostok, Russia, 1999; pp. 109–111. (In Russian)

43. Sayadyan, G.R.; Gonevchuk, V.G.; Gerasimov, N.S.; Khomich, V.G. Geological and isotopic-geochemical basis for basing the age and formation sequence of magmatic rocks of the Krinichnoye gold ore field. In *Mineralogo-Geokhimicheskiye Indikatory Rudonosnosti I Petrogenezisa*; Shcheka, S.A., Ed.; Dal'nauka: Vladivostok, Russia, 1996; pp. 93–105. (In Russian)
44. Sayadyan, G.R. Geology, magmatism, and gold mineralization of South Primorye (the Askold strike-slip fault zone, Sergeevka terrane). In *Metallogeny of the Pacific Northwest (Russian Far East): Tectonics, Magmatism and Metallogeny of Active Continental Margins. Excursion Guidebook*; Khanchuk, A.I., Gonevchuk, G.A., Seltmann, R., Eds.; Dal'nauka: Vladivostok, Russia, 2004; pp. 137–146.
45. Prokopiev, A.V.; Ershova, V.P.; Stockli, D.F. Detrital zircon U–Pb data for Jurassic—Cretaceous strata—Correlations to magmatic arcs of the North East Asian Active Margin. *Minerals* **2021**, *11*, 291. [CrossRef]
46. Koua, K.A.D.; Sun, H.; Li, J.; Li, H.; Xie, J.; Sun, Q.; Li, Z.; Yang, H.; Zang, L.; Mondah, O.R. Petrogenesis of Early Cretaceous granitoids and mafic enclaves: Implications for crust-mantle interaction, tectonic evolution and gold mineralization. *J. Asian Earth Sci.* **2022**, *228*, 105096.
47. Mao, J.; Liu, P.; Goldfarb, R.J.; Goryachev, N.A.; Pirajno, F.; Zheng, W.; Zhou, M.; Zhao, C.; Xie, G.; Yuan, S.; et al. Cretaceous large-scale metal accumulation triggered by post-subductional large-scale extension, East Asia. *Ore Geol. Rev.* **2021**, *136*, 104270. [CrossRef]